Steroids 171 (2021) 108832

Contents lists available at ScienceDirect

Steroids

journal homepage: www.elsevier.com/locate/steroids

Biocatalytic modifications of ethynodiol diacetate by fungi, anti-proliferative activity, and acetylcholineterase inhibitory of its transformed products

Sharifah Nurfazilah Wan Yusop [a,b], Syahrul Imran [b,c], Mohd Ilham Adenan [c,d], Kamran Ashraf [a,b], Sadia Sultan [a,b,*]

[a] Faculty of Pharmacy, Universiti Teknologi MARA Puncak Alam Campus, Bandar Puncak Alam, 42300 Kuala Selangor, Selangor, Malaysia
[b] Atta-ur-Rahman Institute for Natural Product Discovery (AuRins), Universiti Teknologi MARA Puncak Alam Campus, Bandar Puncak Alam, 42300 Kuala Selangor, Selangor, Malaysia
[c] Faculty of Applied Sciences, Universiti Teknologi MARA Shah Alam, 40450 Shah Alam, Selangor, Malaysia
[d] Universiti Teknologi MARA, Pahang Branch, Bandar Tun Abdul Razak, 26400 Jengka, Pahang, Malaysia

A B S T R A C T

The fungal transformations of ethynodiol diacetate (**1**) were investigated for the first-time using *Botrytis cinerea, Trichothecium roseum,* and *R*3-2 SP 17. The metabolites obtained are as following: 17α-Ethynyl-17β-acetoxyestr-4-en-3-one-15β-ol (**2**), 19-nor-17a-ethynyltestosterone (**3**), and 17α-ethynyl-3β-hydroxy-17β-acetoxyestr-4-ene (**4**). The new metabolite, **2** (IC_{50} = 104.8 μM), which has ketone group at C-3, and the β-hydroxyl group at C-15, resulted in an almost equipotent strength with the parent compound (IC_{50} = 103.3 μM) against proliferation of SH-SY5Y cells. The previously reported biotransformed product, **3**, showed almost equal strength to **1** against acetylcholinesterase. Molecular modelling studies were carried out to understand the observed experimental activities, and also to obtain more information on the binding mode and the interactions between the biotransformed products, and enzyme.

1. Introduction

Climates, geographical location, substrate type, and microhabitat are among the factors that affect the distribution of fungi globally [1]. These results in a broad range of their physiologies and metabolic assortments. Bioprospection of other less established settings such as the Antarctic continent offers a unique source of microorganisms and their metabolites, presenting a vast capacity of biotechnological applications [2]. For instance, extracellular enzymes such as chitinase activity were also indicated in Antarctic yeasts isolates [3]. Another good example of biotechnological application of unique microorganisms is the discovery of biotransformation ability of *Mortierella minutissima*. *Mortierella minutissima* is a novel psychrotolerant fungus that is used in the biotransformation of D-limonene [4]. Furthermore, *Chrysosporium pannorum* is a novel psychrotolerant fungus that is used in bioconversion of α-pinene [5]. This is important as microbial transformation supports sustainable uses of resources under defined culture conditions, freeing them from pathological restrictions and seasonal fluctuations. These microbial-catalysed reactions aids in generating diverse organic molecules with complex structures such as steroids, and also boosting up drug discovery process. Ethynodiol diacetate **(1)** is a semi-synthetic steroidal drug. It is a potent progestin that inhibits the ovulation process; therefore, it is used as an oral contraceptive. To date, only one study has published information on the microbial transformation of ethynodiol diacetate. Zafar et al., (2012) reported that the microbial transformation of **(1)** could be achieved by *Cunninghamella elegans*. They also indicated that the biotransformation of ethynodiol diacetate resulted in three new hydroxylated compounds: 17α-ethynylestr-4-en-3β,17β-diacetoxy-6α-ol, 17α-ethynylestr-4-en-3β,17β-diacetoxy-6β-ol, and 17α-ethynylestr-4-en-3β,17β-diacetoxy-10β-ol [6]. In addition to the main role of reproductive regulation, progesterone along with progestin (synthetic progesterone) have shown promising outcomes in animal studies of myelin repair, neurodegeneration, and also recovery of brain damage [7]. Cholinergic function was also improved by treatment with progesterone and 17β-estradiol [8]. It has been demonstrated that amyloid-β levels were significantly reduced in the mice when they are subjected to treatment of cyclic progesterone alone [9].

In a continuation of our work on microbial transformation [10–18], we report here for the first time the microbial transformation of ethynodiol diacetate by *Botrytis cinerea*, *Trichothecium roseum*, and *R*3-2 SP

* Corresponding author at: Faculty of Pharmacy, Universiti Teknologi MARA Puncak Alam Campus, Bandar Puncak Alam, 42300 Kuala Selangor, Selangor, Malaysia.
E-mail address: drsadia@uitm.edu.my (S. Sultan).

https://doi.org/10.1016/j.steroids.2021.108832
Received 10 September 2020; Received in revised form 22 March 2021; Accepted 28 March 2021
Available online 6 April 2021
0039-128X/

17. Ethynodiol diacetate (**1**) along with its biotransformed metabolites were subjected to anti-proliferative activity against SH-SY5Y cells and anti-acetylcholinesterase activity.

2. Experimental

2.1. Chemicals

Ethynodiol diacetate (**ED**) was obtained from Sigma-Aldrich. All chemicals used were of HPLC grade and analytical grade from Merck.

2.2. Microorganisms

The ATCC fungi (*Tricothecium roseum,* and *Botrytis cinerea*) were subcultured on (PDA) plates and stored at 28℃ in an incubator. The Antarctic fungus, *R*3-2 SP 17 was subcultured, and stored at 4℃ in the chiller. Petri dishes were incubated for 5 days for all fungi. Microbial cultures were transferred into a broth medium flask containing freshly prepared sterilised fermentation medium (40 mL in 100 mL flask) from the agar plates.

2.3. Medium preparation and fungal cultivation for biotransformation experiments

All biotransformation experiments for all fungi were set as followed. The fermentation medium was prepared according to a specific recipe; the specific recipe contains the measured ingredients (Glucose (10.0 g), KH_2PO_4 (5.0 g), peptone (5.0 g), yeast extract (5.0 g), NaCl (5.0 g), glycerol (10.0 mL)) in 1.0 L of purified water. The medium was then distributed evenly among conical flasks (100 mL in 250 mL flask). Sterilisation was completed using autoclave. 2.0 L of culture medium for each fungus was prepared. Spores were transferred aseptically into the 250 mL conical flasks containing 100 mL of sterile medium and were incubated for 48 h at 28 °C. The cultures were shaken at 80 rpm on an orbital shaker. Aliquots (300 μL) from the seed flask were transferred aseptically to twenty flasks (for each fungus), and grown for a further 72 h. After 3 days of culture, the substrate solution **(**300 mg/ 8 mL**)** was transferred equally into all the flasks **(**15 mg/ 0.40 mL/ flask**)** under sterilized conditions. The flasks were maintained under the same conditions for an additional 12 days for ethynodiol diacetate.

2.4. HPLC analysis and isolation of the biotransformed products

The fermentation media were extracted three times with ethyl acetate. The organic extract was evaporated under reduced pressure on a rotary evaporator. One mg of the extract was dissolved in 1 mL of methanol (MeOH). The sample was filtered through a nylon membrane filter 0.45 μm. The extracts were analysed using a diode array detector (DAD). The detector was also set to display the absorbance at the following wavelengths: 220, 254, 280, 320 and 360 nm. All analyses were carried out in a reverse phase mode, using a Synergy 4 μm Hydro-RP 80 Å column (150 × 4.6 mm, 4 μm particle size, Phenomenex®, USA) with a guard column filled with the same material. The column temperature was maintained at 36℃. The mobile phase comprises of purified water (solvent A) and acetonitrile (solvent B). The assessment was carried out at a flow rate of 1 mL/min with the following elution gradient: 0 min 10% B, 10 min 46% B, 15 min 70% B, and 20 min 100% B. The qualitative analysis of ED metabolites was carried out by Agilent HPLC-1200 using a 10 μL injection. Purification of sample mixtures from GILSON-PLC 2020 was achieved using Recycling Preparative HPLC (RP-HPLC JAI LC-9103) fitted with JAIGEL ODS-AP, 20 X 250 mm column. Sample (10–70 mg) was injected into the system in a single injection, and the RP-HPLC was set to an isocratic condition of ACN in water (Flow rate: 4 mL/min) with pre-set UV of 220 nm/250 nm depending on the chromatographic profiles of sample mixtures.

2.5. Structure elucidation of biotransformed products

The structure of metabolites was identified by their comprehensive spectral data. Nuclear magnetic resonance (NMR) spectra were completed based on solubility of the samples in deuterated solvents (chloroform-d ($CDCl_3$), acetone-d_6 (CD_3COCD_3), and methanol-d_4 (CD_3OD)) $CDCl_3$ on Bruker Ultra Shield Plus 600 MHz and 500 MHz (Bruker, USA) using a 5 mm probe. All solvents were purchased from Merck. ^{1}H NMR, ^{13}C NMR, DEPT, HMQC, HMBC, COSY, and NOESY spectra were recorded using a 5 mm probe. HRMS analysis was performed on Agilent LC/TOF-MS 6210 mass spectrometer system. IR absorbances (cm^{-1}) were measured on Bruker Tensor II FT-IR spectrophotometer. UV (in nm) absorbances were recorded on Jasco J-815 spectrophotometer.

2.6. Spectroscopic data of biotransformed products

2.6.1. 17α-Ethynyl-17β-acetoxyestr-4-en-3-one-15β-ol: (2)

Yellow-brown residue, yield (percentage yield): 7.00 mg (2.33%); HRMS *m/z*:

$[M + Na]^+$ at *m/z* 379.1872, for $C_{22}H_{28}O_4Na$ (calcd. 379.1885). UV (MeOH) λ_{max} nm (241). IR (MeOH, cm^{-1}): υ = 3418, 2924, 1744, and 1680. ^{1}H NMR (600 MHz, $CDCl_3$, δ, ppm): 5.897 (1H, s, H-4), 4.318 (1H, s, H-15), 2.188 (1H, m, H-16b), 2.010 (1H, m, H-16a), 1.059 (1H, t, *J* = 10.62 Hz, H-14), 2.736 (1H, m, H-2a), 2.169 (1H, m, H-2b), 2.349 (1H, m, H-1a), 1.652 (1H, m, H-1b), 1.961 (1H, m, H-7a), 1.148 (1H, m, H-7b), 1.823 (1H, m, H-11a), 1.448 (1H, m, H-11b), 2.494 (1H, m, H-12a), 2.284 (1H, m, H-12b), 2.116 (1H, m, H-10), 1.487 (1H, m, H-9), 2.458 (1H, m, H-8), 2.326 (1H, m, H-6a), 2.308 (1H, m, H-6b), 1.172 (3H, s, CH_3-18), 2.646 (1H, s, H-21), 2.078 (3H, s, CH_3-25). ^{13}C NMR (151 MHz, $CDCl_3$, δ, ppm): Table 1.

2.6.2. 19-nor-17a-ethynyltestosterone: (3)

White amorphous powder, yield (percentage yield): 20.00 mg (6.67%); HRMS *m/z*: $[M + Na]^+$ at *m/z* 361.2373, for $C_{20}H_{26}O_2Na$ (calcd 321.1830). UV (MeOH) λ_{max} nm (240). ^{1}H NMR (600 MHz, $CDCl_3$, δ, ppm): 5.858 (1H, s, H-4), 1.758 (1H, m, H-15a), 1.305 (1H, m, H-15b), 2.316 (1H, m, H-16a), 2.003 (1H, m, H-16b), 1.565 (1H, m, H-14), 2.354 (1H, m, H-2a), 2.287 (1H, m, H-2b), 2.265 (1H, m, H-1a), 1.552 (1H, m, H-1b), 1.848 (1H, m, H-7a), 1.083 (1H, m, H-7b), 1.931 (1H, m, H-11a), 1.263 (1H, m, H-11b), 1.883 (1H, m, H-12a), 1.624 (1H,

Table 1
^{13}C NMR data for compounds **1**–**4.**

No.	1	2	3	4
1	23.38	26.02	26.58	22.65
2	34.99	37.32	36.50	35.14
3	70.28	199.87	199.61	64.54
4	119.98	124.84	124.61	121.85
5	144.74	167.15	166.51	145.27
6	31.36	36.51	35.47	32.98
7	25.72	30.79	30.66	31.26
8	41.21	35.1	41.04	41.13
9	49.40	48.77	49.12	49.42
10	41.65	37.51	42.56	42.02
11	25.21	23.19	26.21	26.20
12	32.91	35.12	32.43	30.35
13	47.71	47.27	46.86	47.75
14	47.67	53.06	49.16	47.70
15	23.39	66.73	22.88	23.43
16	37.27	41.38	38.82	37.28
17	84.49	84.55	79.71	84.53
18	13.42	15.95	12.60	13.43
20	83.33	83.28	87.26	83.35
21	78.48	75.47	74.17	74.80
22	169.50	169.55	–	–
23	21.40	21.40	–	–
24	170.85	–	–	169.61
25	21.40	–	–	21.45

m, H-12b), 2.112 (1H, td, $J = 4.62, 10.32$ Hz, H-10), 0.914 (1H, m, H-9), 1.352 (1H, m, H-8), 2.422 (1H, dt, $J = 5.88, 10.02$ Hz, H-6a), 2.273 (1H, m, H-6b), 0.936 (3H, s, CH_3-18), 2.603 (1H, s, H-21). ^{13}C NMR (151 MHz, $CDCl_3$, δ, ppm): Table 1.

2.6.3. 17α-ethynyl-3β-hydroxy-17β-acetoxyestr-4-ene: (4)

White residue, yield (percentage yield): 7.96 mg (2.65%); HRMS *m/z*: [M + H] + at *m/z* 365.4188, for $C_{22}H_{30}O_3Na$ (calcd. 365.2093). UV (MeOH) λ_{max} nm (240). ^{1}H NMR (600 MHz, $CDCl_3$, δ, ppm): 4.159 (1H, m, H-3), 5.581 (1H, d, $J = 4.5$ Hz, H-4), 1.363 (1H, m, H-15a), 1.776 (1H, m, H-15b), 2.011 (1H, m, H-16a), 2.754 (1H, m, H-16b), 2.036 (1H, m, H-2a), 2.262 (1H, m, H-2b), 1.406 (1H, m, H-1a), 1.845 (1H, m, H-1b), 1.148 (1H, m, H-7a), 1.961 (1H, m, H-7b), 1.227 (1H, m, H-11a), 1.942 (1H, m, H-11b), 1.578 (1H, m, H-12a), 1.803 (1H, m, H-12b), 1.729 (1H, m, H-10), 0.815 (1H, m, H-9), 1.286 (1H, m, H-8), 1.703 (1H, m, H-6a), 1.889 (1H, m, H-6b), 0.927 (3H, s, CH_3-18), 2.610 (1H, s, H-21), 2.064 (3H, s, CH_3-25). ^{13}C NMR (151 MHz, $CDCl_3$, δ, ppm): Table 1.

2.7. Anti-proliferative study of biotransformed products against human neuroblastoma cells (SH-SY5Y cell line)

Anti-proliferative activity of biotransformed metabolites were evaluated against SH-SY5Y cells (human neuroblastoma cells) by using the MTT (3-(4, 5-dimethyl thiazol-2yl)-2, 5-diphenyl tetrazolium bromide) assay. SH-SY5Y cells were maintained in Nacalai Tesque Minimal essential medium (MEM) containing 4-(2-hydroxyethyl)-1-piperazineethanesulfonic acid (HEPES) supplemented with F-12 K nutrient mixture, 10% (v/v) foetal bovine serum, and 1% penicillin–streptomycin in T175 flasks. The cells were kept at 37 °C in humidified 5% CO_2 incubator and they were passaged every three days. Cells were introduced into 96-well plates at a concentration of 25 000 cells/well and incubated for 24 h. After 24 h, medium was removed, and cells were treated for 24 h with various concentrations of the biotransformed compounds (3.906, 7.813, 15.625, 31.250, 62.5, 125, 250 and 500 μM). Twenty-four hours later, 20 μL of MTT solution (5 mg dissolved in 1 mL PBS) was added into each well including controls and incubated for another 4 h at 37 °C. Next, 100 μL dimethyl sulfoxide (DMSO) was added to each well to dissolve resultant formazan crystals. Reduction of MTT to formazan crystals by mitochondrial dehydrogenase which is present in viable cells was visualized by the development of blue formazan product. The absorbance was read at 570 nm with a microplate reader SPECTROstar Nano (BMG LABTECH). Cisplatin was used as positive control for human neuroblastoma cells, whereas DMSO was added in the negative control instead of compounds (Table 2).

Cell proliferation inhibition (%) = 100-{(As-Ab)/ (Ac-Ab)} x100

Where,

As = Absorbance value of sample compound

Ab = Absorbance value of blank

Ac = Absorbance value of control

Table 2
In-vitro anti-proliferative activities of **ED**, and its metabolites against human neuroblastoma cell line, SH-SY5Y.

Compound	IC_{50} (μM)
1	103.30 ± 0.03776
2	104.80 ± 0.07355
3	169.30 ± 0.07735
4	206.80 ± 0.03967
Cisplatin [b]	0.61 ± 0.09010

Results are expressed as IC_{50} values (μM). IC_{50} ± S.E.M are also given. All value is the mean of three replications.
[b]Control used in the assays.

2.8. Acetylcholinesterase inhibition assay

2.8.1. In-vitro anti-acetylcholinesterase activities of biotransformed products and their precursors

Slight modification to Ellman's developed spectrophotometric method was used for measurement of AChE inhibiting activity of biotransformed compounds. Physostigmine was used as a reference for AChE inhibitor and measurement of anticholinesterase activity was done using 5, 5′-Dithio-bis (2-nitrobenzoic) acid (DTNB). The reference, physostigmine, and all the test samples were dissolved in a buffer prior to assay at a stock concentration of 3.125 mM and serial dilution was done accordingly. In brief, 190 μL DTNB, 20 μL of sample solution, and 20 μL of AChE enzyme solution were added using multichannel automatic pipette) into a 96-well microplate and incubated for 10 min at 37 °C. Next, addition of 20 μL acetylcholine iodide (substrate) initiated the reaction. The reaction of thiocholines and DTNB catalysed by enzymes gave rise to the formation of the yellow 5-thio-2-nitrobenzoate, which signifies the degree of hydrolysis of acetylcholine iodide. The degree of hydrolysis of acetylcholine iodide was measured using a microplate reader SPECTROstar Nano (BMG LABTECH), where the absorbance was read kinetically for 15 min at 412 nm. Reaction rates for the samples to the blank were compared in order to measure enzyme activity of the isolated biotransformed products. GraphPad Prism was used to determine IC_{50} values.All the samples were tested in triplicates, and the results were expressed as mean ± SEM.

Percentage inhibition (%) =

$$\frac{\text{Absorbanceofcontrol} - \text{Absorbanceoftestsample}}{\text{Absorbanceofcontrol}} \times 100\%$$

2.8.2. In-silico studies of acetylcholinesterase inhibition

The crystal structure of recombinant human AChE (PDB ID: 4EY7) was obtained from the Research Collaboratory for Structural Bioinformatics (RCSB) Protein Data Bank. The structure contained a known co-crystallized inhibitor Donepezil. The 3D structure of recombinant human AChE (rhAChE) was prepared using BIOVIA Discovery Studio Visualizer Version 17.2.0.16349. The preparation of the structure includes the process of deletion of ligand, removal of all water molecules, addition of the missing hydrogen atoms, and minimisation of energy. Validation of the docking protocol was performed in order to ensure its reliability for later analysis of the studied compounds. Donepezil was extracted from the co-crystal ligand from the PDB file and later re-docked to the co-crystal recombinant human AChE protein. The computation was performed for the root mean squared deviation (RMSD) of the atomic position between the original orientation of the co-crystal ligand and the re-docked ligand. The value is deemed acceptable if the RMSD value is less than or equal to 2.0. The ligands (two most potent biotransformed compounds) were prepared using ChemDraw Ultra Version 12.0.2.1076 and ChemDraw 3D Pro Version 12.0.2.1076. Grid box was prepared to maintain coverage of the active site of a recombinant human with a dimension of 50X50X50 Å (X, Y, and Z axes of 10.634, −56.163, −23.873, respectively. Molecular docking was consequently performed using AutoDock 4.2 using refined protein and ligands. Finally, AutoDock 4.2 was run continually to get best 150 different docked conformational poses against a target molecule. The parameters such as inhibition constant, binding energy and intermolecular energy for the two most potent biotransformed products were studied. The three-dimensional structure of protein–ligand interaction was created and visualised using BIOVIA Discovery Studio Visualizer Version 17.2.0.16349.

3. Results and discussion

3.1. Structure elucidation

Microbial transformation of ethynodiol diacetate ($C_{24}H_{33}O_3$) (**1**)

using *Botrytis cinerea*, and *Trichothecium roseum* are reported here for the first time. Fermentation of **1** with *B. cinerea* yielded one new metabolite **2** (Fig. 1). Biotransformation of **1** by *T. roseum* yielded one known metabolite **3** (Fig. 1). A known compound **4** was obtained from biotransformation of **1** with the Antarctic fungus, *R*3-2 SP 17 (Fig. 1).

The isolated new metabolite **2** is obtained as yellow–brown residue from RP-HPLC (60% ACN in water with pre-set UV of 250 nm).The molecular formula of **2** was established as $C_{22}H_{28}O_4$ as supported by the presence of adduct ions surfacing at *m/z* 379.1872 (calcd. 379.1885) and and *m/z* 735.3874 (calcd. 735.3873) corresponding to sodium adducts $[M + Na]^+$ and $[2\ M + Na]^+$, respectively in the (+) HRMS analysis. HPLC-DAD analysis showed the UV spectrum having absorption at 241 nm. The IR spectrum of **2** displayed absorptions at 3418, 2924, 1744, and 1680 cm^{-1} indicative for hydroxyl and conjugated carbonyl functionalities, respectively. The ^1H NMR spectrum of metabolite **2** displayed two methyl groups where both methyls appeared as singlets at δ 1.172 and δ 2.078, assigned to CH_3-18 and CH_3-23, respectively. The loss of one of the methyl groups when compared to the substrate, **1** suggested removal of acetate at C-3 leading to ketone formation. The loss of one methylene proton signals was in line to an additional downfield signal (δ 4.318), suggesting the hydroxylation of the methylene group. The ^{13}C NMR and DEPT spectra of the biotransformed product gave a total of 22 carbon signals. The HMQC correlations presented the proton signal at δ 5.897, which corresponded to an olefinic methine carbon signal at δ 124.84 (C-4). The olefinic methine proton and carbon signals have become deshielded and this could be due to an adjacent carbonyl group. Hence, a carbonyl group at C-3 is established by the occurrence of downfield quaternary carbon value at δ 199.73. The loss of one methylene carbon signal and the presence of a downfield signal at δ 66.73 was attributed to the C-11 methine, which gave additional evidence of the presence of an OH group at this carbon. Methyl carbons resonated at δ 15.95, and δ 21.40 and they were attributed to C-18 and C-19 methyl carbons respectively. The position of carbonyl carbon was assigned at C-3 (δ 199.87) based on HMBC correlations of H-1a (δ 1.652) and H-1b (δ 2.349) with C-3 (δ 199.87). HMBC correlations of C-4 proton (δ 5.897) to C-2 (δ 37.32) and C-6 (δ 36.51) also supported the assignment of ketonic carbonyl carbon at C-3. The position of the hydroxyl group was assigned at C-15 (δ 66.73) was also based on the key HMBC correlations of H-16a (δ 2.010) with C-15 (δ 66.73), and H-15 (δ 4.318) with C-13 (δ 47.27) (Fig. 2). In the COSY spectrum, H-15 (δ 4.318) showed correlations with H-14 (δ 1.059), H-16a (δ 2.010) and H-16b (δ 2.188). The stereochemistry of the hydroxyl group at C-15 was deduced to be β on the basis of NOESY correlations between H-15 (δ 4.318), and H-14 (δ 1.059). Therefore, a β-OH was placed at C-15. Thus, the structure of the new compound was characterized as 17α-Ethynyl-17β-acetoxyestr-4-en-3-one-15β-ol (Fig. 3).

Fermentation of **1** with *T. roseum* yielded a known product (as the main transformation product). The metabolite **3** was characterized as norethisterone based on detailed spectrometric studies. Compound **3** was previously reported by Zafar et al. (2012) where it was obtained via biotransformation technique of using plant cell suspension cultures of *Ocimum basilicum* (20 mg product yield and required 35 days for the whole process) & *Azadirachta indica*. (Yield not disclosed, and also required 30 days for the whole process). Freudenthalet. al., 1977 reported that incubation of **1** with rat and human liver cells has also resulted in the formation of metabolite **3**. To date, no formation of **3** via microbial transformation has been reported. Our findings have shortened the process to about half of the time reported with comparable yield, used less starting material, and no photoperiod required when compared with the studies done by Zafar et al. (2012). Metabolite **3**, isolated as a white amorphous powder from the isocratic condition of 50% ACN in water with pre-set UV of 250 nm on RP-HPLC. The HRMS analysis provided a $[M + Na]^+$ at *m/z* 321.6121 which is consistent with $C_{20}H_{26}O_2Na$ formula (calcd 321.1830). The UV spectrum displayed an absorption at 240 nm. The IR spectrum of **3** exhibited absorption bands at 3400 (OH), 3300 (C ≡ CH), 1650 (C═O), and 1445 (C-H_2 bending) cm^{-1}. The ^1H NMR spectrum of **3** was remarkably different from the substrate, in many aspects, especially the loss of C-3 methine, C-23 methyl, and C-25 methyl protons. The C-4 methine proton resonated at a downfield shift δ 5.858, instead of δ 5.350. The disappearance of the C-23 and C-25 methyl signals furthers suggested the hydrolysis of the C-3 and C-17 ester groups. A quaternary carbon signal at δ 199.61, and a downfield methine signal at δ 124.61 exhibited in the ^{13}C NMR spectrum were assigned to C-3 and C-4, respectively, thus providing evidence for the presence of carbonyl signal at C-3. An upfield carbon signal was found resonating at δ 79.71, and this was attributed to quaternary C-17 in the ^{13}C NMR spectrum of metabolite **3,** which further supported hydroxylation has occurred. In the HMBC spectrum of **3**, the C-1 methylene protons (δ 1.552, δ 2.265) showed ^3J heteronuclear couplings with C-3 (δ 199.91). The C-6 methylene protons (δ 2.273, δ 2.422) showed ^2J heteronuclear couplings with C-5 (δ 166.51). Changes to C-17 was supported by the ^3J heteronuclear couplings of C-14 proton (δ 1.565), and C-15 proton (δ 1.758) with C-17 (δ 79.71). C-17 (δ 79.71) also have ^2J heteronuclear couplings with C-18 methyl protons (δ 0.936) and C-16

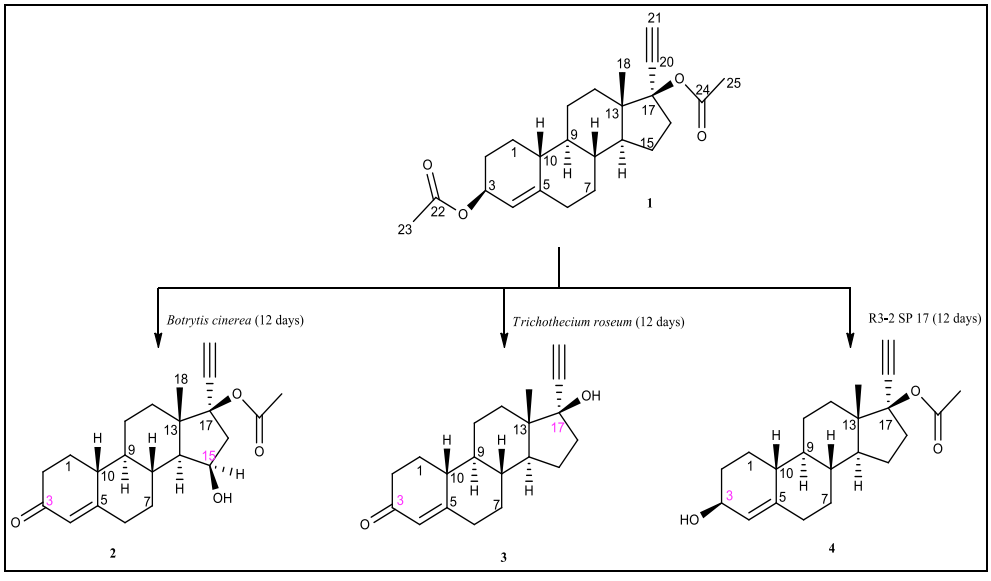

Fig. 1. Biotransformation of ethynodiol diacetate (**1**) with *Botrytis cinerea, Tricothecium roseum,* and *R*3-2 SP 17.

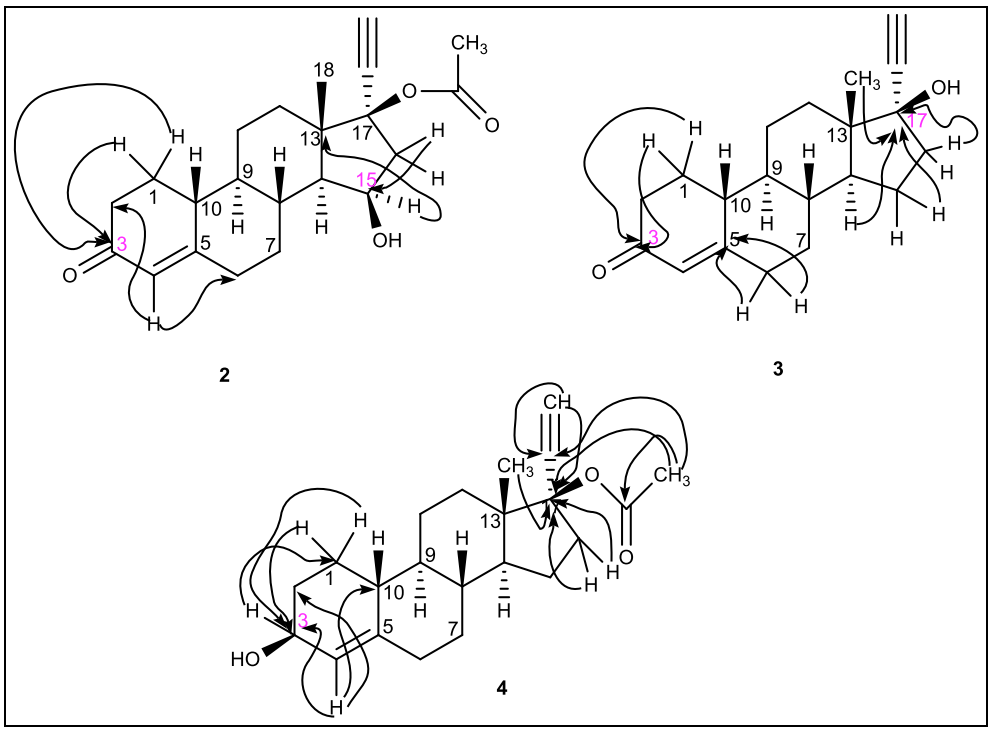

Fig. 2. Key HMBC correlations in metabolites **2**, **3,** and **4.**

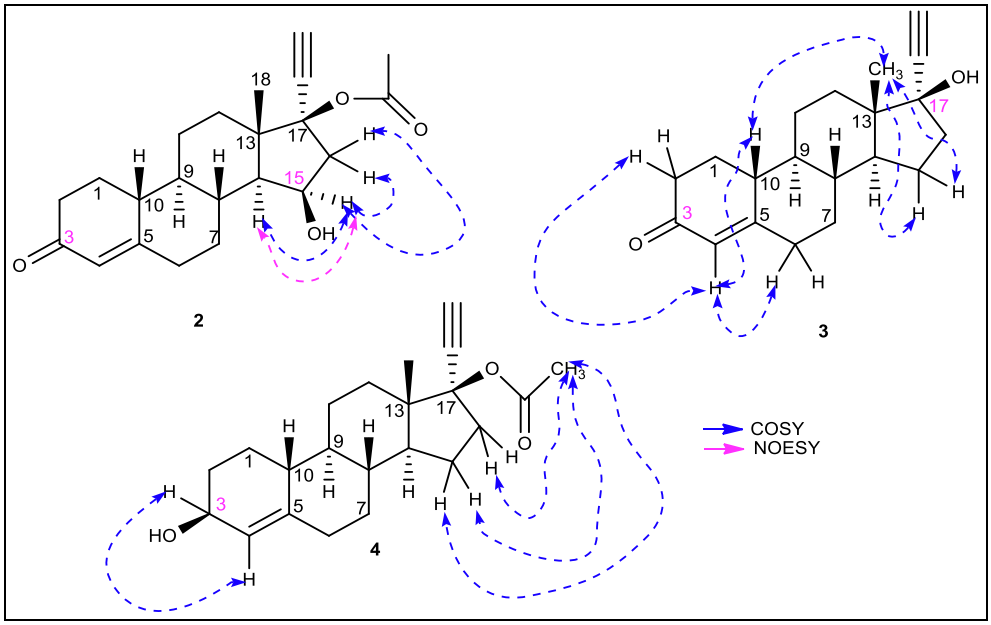

Fig. 3. Key COSY and NOESY correlations in metabolites **2**, **3,** and **4.**

proton (δ 2.003) (Fig. 2). In the COSY spectrum, C-4 methine proton which resonated at δ 5.858, showed cross-peaks with C-2 proton (δ 2.287), C-6 proton (δ 2.422), and C-10 methine proton (δ 2.112). The experiment also showed C-18 methyl protons has homonuclear couplings with H-10 (δ 2.109), and C-15 methylene protons (δ 1.305, δ 1.758) (Fig. 3). In 1951, norethisterone or 19-nor-17a-ethynyltestosterone was first synthesized in the lab of Carl Djerassi, marking the chemical birthday of the pill [19]. Norethisterone is a progestin that is used as oral contraceptive pills. Minami, Kosugi, Suganuma, Yamanaka, & Kusuki (2013) reported that norethisterone induces apoptosis in human endometriotic stromal cells, and have anti-proliferative activity towards the cells [20]. Norethisterone and medroxyprogesterone acetate are significantly metabolised in human cervical tissue although at lesser degree than progesterone [21]. The steroid norethisterone is also one of the examples of novel autophagy inducers apart from oxaprozin, methyltestosterone, and zidovudine [22].

Fermentation of **1** with *R*3-2 SP 17 yielded 7.96 mg of metabolite **4** as the main transformation product. Metabolite **4** was identified as 2 based on the spectrometric studies and evaluation of the reported data by Zafar et al. (2012) as a biotransformation product of **1** by plant cell suspension cultures of *Ocimum basilicum*. The research team also reported that they only managed to obtain 3.5 mg of product yield **4** from the use of 600 mg

of the substrate and required a total of 35 days for the whole process. Again, the findings here have shortened the process to about half of the time reported, used less starting material and yielded more of the product when compared with the studies done by Zafar et al. (2012). Our technique has no photoperiod required. Another research was done in 1977 by Freudenthalet. al. has described the formation of metabolite **4** by incubation of **1** with rat and human liver cells (Freudenthalet. al., 1977, as cited in Zafar et al., 2012). To date, no formation of **4** via microbial transformation has been reported. Metabolite **4** was isolated as white residue from the isocratic condition of 80% ACN in water with pre-set UV of 220 nm on RP-HPLC. The HRMS analysis of the metabolite displayed a $[M + Na]^+$ at *m/z* 365.4188 which is consistent with $C_{22}H_{30}O_3Na$ formula (calcd. 365.2093). This showed the loss of 42 a.m.u, when compared to **1**, and this was indicative of the modification of the acetate region in the transformed product. This was further supported by the existence of adduct ions appearing at *m/z* 707.1213 (calcd. 707.4288) that also corresponds to sodium adduct $[2\,M + Na]^+$. The UV spectrum showed an absorption at 240 nm. The IR spectrum exhibited absorption bands at 3415 (OH), 1648 (C═O) and 1598 (C═C) cm^{-1}. The absence of δ 5.233 signal of starting material in the ^{1}H NMR spectrum that is a proton geminal signal to ester group at C-3 suggests modification might have occurred at this region. However, the ^{1}H NMR spectrum of compound **4** displayed a broad singlet at δ 4.159 and also another broad singlet at δ 5.581 which are attributed to C-3 and C-4, respectively. The presence of a singlet for methyl group at δ 2.064 (H-25), indicates that the ester at C-17 is still intact. The missing methyl group at C-3 indicates hydrolysis of the C-3 ester into an –OH. Another methyl group that still remains is represented by a singlet at δ 0.927 that is due to the C-18 methyl group. The rest of the spectrum was almost similar to the **1**. The ^{13}C NMR spectra exhibited the presence of two methyls, eight methylene, seven methine and five quaternary carbons. Two quaternary carbon signals at δ 84.53 and δ 83.35 were assigned to C-17 and C-20, respectively. This further confirms the C-17 ester group is still intact and the loss of an ester group is due to hydrolysis of C-3 ester into an –OH. The position and hydrolysis of C-3 ester into an –OH was concluded from distinct assignments of carbons and protons that were made through the analysis of HMQC, HMBC and COSY outcomes. The cross-peaks in the HMBC spectrum further validated the hydrolysis of the ester group at C-3 into an –OH. In the HMBC spectrum, Me-25 protons (δ 2.064) showed heteronuclear correlations with C-17 (δ 84.53), C-20 (δ 83.35), and C-24 (δ 169.61). Along with the assignments of protons and carbons in the HMQC spectrum, this confirms that the C-17 ester is still present. C-17 also exhibited ^3J correlations with H-18 (δ 0.927) and H-21 (δ 2.610) protons, while also having a ^2J correlation with C-16 methylene protons (δ 2.011, δ 2.754). H-21 was also seen having a ^2J correlation with C-20 (δ 83.35). The HMBC spectrum also displayed ^3J correlations of H-3 (δ 4.159) with C-1 (δ 22.65), while C-1 protons (δ 1.406, δ 1.845) also have ^3J correlations with C-3 (δ 64.54). C-4 proton (δ 5.581) was observed to have ^3J correlations with C-2 (δ 35.14) and C-10 (δ 42.02), while also having a ^2J correlation with C-3 (δ 64.51). These too supported no C-3 ester group correlation detected as the C-3 ester group has hydrolysed into –OH and the ester at C-17 is still intact (Fig. 2). The COSY spectrum revealed the presence of cross-peaks between H-3 (δ 4.159) to H-4 (δ 5.581) and these were indicative of the closeness of these protons. C-25 methyl protons have correlations with H-15 methylene protons (δ 1.363, δ 1.776) and one of the H-16 methylene protons (δ 2.754). These too verified that C-17 ester group remains and the hydrolysis of C-3 into –OH as no correlation of ester detected at C-3 region (Fig. 3).

3.2. Anti-proliferative activity of biotransformed products against human neuroblastoma cell line, SH-SY5Y

Sex steroid hormones such as estrogens, androgens, and progesterones (progestins included) have activities on cell differentiation, cell proliferation, and homeostasis [23]. According to the authors, the study of sex steroid hormone neurobiology involves the use of human neuroblastoma SH-SY5Y cells as part of experimental cell models.

In the search of new active compounds with prospective anti-tumour activity, ethynodiol diacetate (**1**) and its metabolites were evaluated for their anti-proliferative activity against human neuroblastoma cell line, SH-SY5Y.

The neuronal cells, SH-SY5Y, were exposed to the parent compound, **1**, and its purified biotransformed products. Removal of acetate and formation of OH-group at C-3 in **4** has caused a major loss of activity against SH-SY5Y, giving rise to the least active biotransformed metabolite of ethynodiol diacetate (IC_{50} = 206.8 μM). The new metabolite, **2** (IC_{50} = 104.8 μM), which has ketone group at C-3, and the β-hydroxyl group at C-15, resulted in an almost equipotent strength with the parent compound (IC_{50} = 103.3 μM). On the other hand, the removal of C-3 and C-17 acetate, and the formation of the β-hydroxyl group at C-17 led to a significant loss of anti-proliferative activity against SH-SY5Y in **3** (IC_{50} = 169.30 μM). It is interesting to note the trend in activities of **2** and **3**, as both have C-3 acetate removal, but with additional hydroxylation at different positions. An extra removal of C-17 acetate and formation of OH-group at C-17 in **3** is shown to be unfavourable to anti-proliferative activity.

3.3. Acetylcholinesterase inhibition assay

3.3.1. In-vitro anti-acetylcholinesterase activities of biotransformed products and their precursor

Depletion of acetylcholine level is associated with a malfunction of the cholinergic neurotransmission leading to loss of memory or intellectual abilities in Alzheimer's disease (AD) patients. Elevation of acetylcholine level at synaptic junctions can be achieved via inhibition of acetylcholinesterase. The elevated level of acetylcholinesterase amplifies the cholinergic transmission which could lead to improvement of cognitive function in AD patients. Octohydroaminoacridine succinate is one of the new acetylcholinesterase inhibition therapies that is currently in phase III of Alzheimer's disease drug development is [24]. To date, only drugs of this class are approved by the Food and Drug Administration (FDA). Donepezil, galantamine, and rivastigmine are the three acetylcholinesterase inhibitors approved by the FDA [25].

To determine the inhibitory potential of the ethynodiol diacetate analogues, the inhibitory activities of **1** and its biotransformed products (**2, 3,** and **4**) were evaluated against acetylcholine (AChE) using the modified Ellman's method [26]. Physostigmine was used as a reference inhibitor for comparison purposes. Table 3 summarises IC_{50} values of biotransformed products of **ED** for the inhibition of AChE.

The impact of the modification pattern of the starting material on the inhibition activity of acetylcholinesterase of isolated biotransformed derivatives tested in this assay was examined. None of the transformed metabolites of **1** has improved AChE inhibitory activity than the starting material, **1**, under the same experimental conditions. Removal of both acetates and formation of ketone at C-3 and introduction of the hydroxyl group at C-17 in the isolated biotransformed product of **3** (IC_{50} = 27.22 μM) proved to be an ineffective strategy to increase enzyme inhibition. A minor change to starting material, which involves the removal of

Table 3
In-vitro anti-acetylcholinesterase activities of **ED**, and its metabolites.

Compound	IC_{50} (μM)
1	24.44 ± 0.04704
2	40.19 ± 0.05158
3	27.22 ± 0.04102
4	42.65 ± 0.06331
Physostigmine [b]	0.067 ± 0.04448

Results are expressed as IC_{50} values (μM). IC_{50} ± S.E.M are also given. All value is the mean of three replications.
[b] Positive control used in the assays.

acetate, and the introduction of a β-hydroxyl group at C-3 resulted in the formation of **4**. Further compound **4** exhibited the weakest AChE inhibition (IC_{50} = 42.65 μM) among the isolated biotransformed products as compared to **3**, and its starting material, **ED**. Ketone formation at C-3 and hydroxylation at C-15 in **2** was also detrimental to acetylcholinesterase inhibition strength (IC_{50} = 40.19 μM).

B. *In-silico* (molecular modelling) studies of acetylcholinesterase

Molecular modelling studies of the enzyme-ligand binding interactions of the stating material, and biotransformed products, within the active site of rhAChE produces a structural insight into the inhibition mechanism of biotransformed products.

Biotransformed metabolites of **1** interacted with various residues via formation of multiple hydrogen bonds, and non-bonding interactions in the docked rhAChE-ligand complex. Hydrogen bonding between a protein, and its ligands is important in molecular recognition as they contribute to directionality, and specificity of interactions [27]. The AChE residues found involved in hydrogen bonds in **1** were VAL 294, PHE 295, TRP 86, HIS 447, and GLY 48 (Fig. 4 (1)**A.**). GLY 126, TYR 133, TYR 337, and TYR 124 were the AChE residues found associated with hydrogen bonds in **2** (Fig. 4 (2)**B.**). Biotransformed metabolite **3** has hydrogen bond interactions with the AChE residues TYR 133, TYR 124, and GLY 120 (Fig. 4 (3)**C.**). Lastly, metabolite **4** has hydrogen bond interactions with the AChE residues TYR 133, TYR 337, ALA 127, GLY 126, GLY 121 and GLY 120 (Fig. 4 (4)**C.**).

As acetylcholinesterase inhibitors, attachment of **1**–**4** at acetylcholinesterase inhibitors at binding site restrains the interaction of acetylcholine molecule with binding site residues leading to impairment of hydrolysis reaction. As acetylcholine concentration intensifies, this would eventually lead to an increase in cholinergic transmission [28]. The simulations suggest that ligand interactions of **1** with residues VAL 294, PHE 295, TRP 86, HIS 447, and GLY 48 of rhAChE. These residues are parts of binding pocket 78 (P78), which is also known as β-anionic site of AChE are significant for its inhibitory activity [29]. Although **3** has hydrogen bond interactions with residues that are also part of P78, the smaller number of hydrogen bond interactions formed in **3** when compared to **1** may have caused the slight loss of activity. In this study, it was also observed only in **3** that the carbonyl group was located nearby to one of the catalytic triad residues, HIS 447 of acetylcholinesterase. HIS 447 along with SER 203 are believed to be directly involved in the forming and breaking of bond for the natural mechanism[30]. The imidazole group of HIS 447 acts as a catalytic base, accepting one proton transferred from SER 203 where the SER 203 functions as a nucleophilic attacking site [31]. The result of **3** suggests that a nucleophilic can occur between SER 203 and carbonyl group in the inhibitor with the presence of HIS 447 nearby. However, this nucleophilic attack is not observable through molecular docking, and no interaction is observed. In previous study, it was reported that the catalytic serine residue of acetylcholinesterase promotes a nucleophilic attack in the carbonyl group of physostigmine [31]. PHE 295 hydrogen bond interaction was observed in **1**. In addition, PHE 295 is one of the main residues in the acyl binding pocket, and it is responsible for interacting with acetyl group [32]. PHE 295 along with PHE 297 function as gatekeepers that limit the dimension of substrates that can enter the active site [33]. The loss of this interaction in **2**, **3**, and **4** implies the decline in inbition of acetylcholinesterase. Thus, all these residues must be considered for the development of rational structure-based acetylcholinesterase inhibitors with

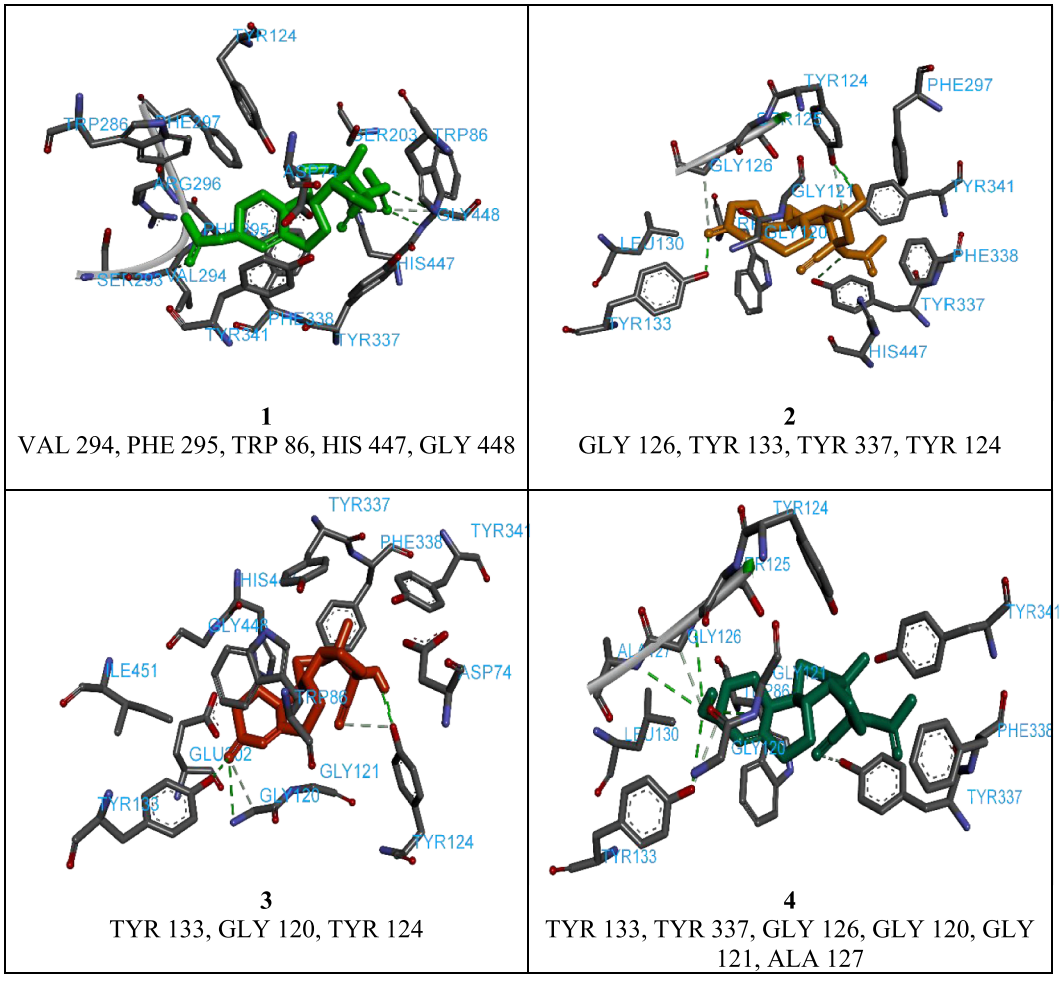

Fig. 4. Key hydrogen bonding interactions between AChE, and compounds **1**, **2**, **3,** and **4.**

increased potency and high specificity.

4. Conclusions

Microbial transformation of compound **1** yielded metabolites **2**, **3**, and **4** respectively with *Botrytis cinerea*, *Trichothecium roseum*, and *R*3-2 SP 17. Compound **2** was found to be new, while **3** and **4** were found to be known products. The use of psychrotolerant fungus as biocatalytic agent of **1** was reported here for the first time, resulting a significant, improved yield of **3**, and **4** than previous reported technique. Among all the tested biotransformed compounds, the new biotransformed product, **2** is almost as potent as parent compound, **1** for anti-proliferative activity against SH-SY5Y tumour cell line. Compound **3** has comparable acetylcholinesterase inhibition as **1**. This is further supported by the binding mechanism of **1**, and **3** into the structure of rhAChE, which were examined through molecular docking studies. The activities reported here deserve to be put into consideration as they are good illustrations in supporting the application of microbial transformation as a viable method of future development of anti-proliferative drug candidates, and acetylcholinesterase inhibitors.

Declaration of Competing Interest

The authors declare that they have no known competing financial interests or personal relationships that could have appeared to influence the work reported in this paper.

Acknowledgements

We would like to acknowledge Universiti Teknologi MARA for the financial support under the reference number 600-IRMI 5/3 LESTARI (025/2019), Faculty of Pharmacy, UiTM and Atta-ur-Rahman Institute For Natural Product Discovery (AuRIns), University Teknologi Mara (UiTM) for outstanding research facilities. Author would also like to acknowledge Associate Prof Dr. Siti Aisah Binti Alias (University MALAYA) for allow us to use Antarctic fungus R3-2 SP 17 for fermentation of ED.

Appendix A. Supplementary data

Supplementary data to this article can be found online at https://doi.org/10.1016/j.steroids.2021.108832.

References

[1] C. Manoharachary, I.K. Kunwar, A.B. Rajithasri, Advances in applied mycology and fungal biotechnology *, KAVAKA. 43 (2014) 79–92.
[2] S. Castro-Sowinski (Ed.), Microbial Models: From Environmental to Industrial Sustainability, Springer Singapore, Singapore, 2016.
[3] M. Carrasco, J. Rozas, S. Barahona, J. Alcaíno, V. Cifuentes, M. Baeza, Diversity and extracellular enzymatic activities of yeasts isolated from King George Island, the sub-Antarctic region, BMC Microbiol 12 (1) (2012) 251, https://doi.org/10.1186/1471-2180-12-251.
[4] M. Trytek, J. Fiedurek, A novel psychrotrophic fungus, Mortierella minutissima, for D-limonene biotransformation, Biotechnol Lett 27 (3) (2005) 149–153, https://doi.org/10.1007/s10529-004-7347-x.
[5] M. Trytek, K. Jedrzejewski, J. Fieudurek, Bioconversion of α – pinene by a novel cold – adapted fungus Chrysosporium pannorum, J. Ind. Microbiol. Biotechnol. (2015) 181–188. doi:10.1007/s10295-014-1550-0.
[6] S. Zafar, S. Yousuf, H.A. Kayani, S. Saifullah, S. Khan, A.M. Al-Majid, M. I. Choudhary, Biotransformation of oral contraceptive ethynodiol diacetate with microbial and plant cell cultures, Chem. Cent. J. 6 (1) (2012), https://doi.org/10.1186/1752-153X-6-109.
[7] R. Sitruk-Ware, M. El-Etr, Progesterone and related progestins: potential new health benefits, Climacteric 16 (sup1) (2013) 69–78, https://doi.org/10.3109/13697137.2013.802556.
[8] R.B. Gibbs, Effects of gonadal hormone replacement on measures of basal forebrain cholinergic function, Neuroscience 101 (4) (2000) 931–938, https://doi.org/10.1016/S0306-4522(00)00433-4.
[9] J.C. Carroll, E.R. Rosario, A. Villamagna, C.J. Pike, Continuous and Cyclic Progesterone Differentially Interact with Estradiol in the Regulation of Alzheimer ' s Disease Mice, Endocrinology 151 (2010) 2713–2722, https://doi.org/10.1210/en.2009-1487.
[10] S. Sultan, M.I. Choudhary, S.N. Khan, U. Fatima, M. Atif, R.A. Ali, A.U. Rahman, M. Q. Fatmi, Fungal transformation of cedryl acetate and alpha-glucosidase inhibition assay, quantum mechanical calculations and molecular docking studies of its metabolites, Eur. J. Med. Chem. 62 (2013) 764–770, https://doi.org/10.1016/j.ejmech.2013.01.036.
[11] S.A.A. Shah, S. Sultan, H.S. Adnan, A whole-cell biocatalysis application of steroidal drugs, Orient. J. Chem. 29 (2013) 389–403. doi:10.13005/ojc/290201.
[12] S. Erum, S. Sultan, S.A.A. Shah, M. Ashraf, M.I. Choudhary, Microbial Oxidation of Finasteride With Macrophomina Phaseolina(Kucc 730), Int. J. Pharm. Pharm. Sci. 9 (2017) 17. doi:10.22159/ijpps.2017v9i11.13576.
[13] M.I. Choudhary, S. Sultan, S. Jalil, S. Anjum, A. Rahman, H.-K. Fun, Atta-ur-Rahman, Microbial Transformation of Mesterolone, C&B 2 (3) (2005) 392–400, https://doi.org/10.1002/cbdv.200590019.
[14] M. Atif, S.A.A. Shah, S. Sultan, M.I. Choudhary, Solid phase microbial fermentation of anabolic steroid, dihydrotestosterone with ascomycete fungus fusarium oxysporum, Int. J. Pharm. Pharm. Sci. 7 (2015) 104–107.
[15] S. Sultan, M. Zaimi Bin Mohd Noor, E.H. Anouar, S.A.A. Shah, F. Salim, R. Rahim, Z.B.K. Al Trabolsy, J.F.F. Weber, Structure and absolute configuration of 20β-hydroxyprednisolone, a biotransformed product of prednisolone by the marine endophytic fungus penicilium lapidosum, Molecules. 19 (2014) 13775–13787. doi:10.3390/molecules190913775.
[16] M.I. Choudhary, S. Sultan, M. Atif, S.A.A. Shah, S. Erum, Atta-ur-Rahman, Microbial Metabolism of an anti-HIV and anti-malarial natural product andrographolide, Int. J. Pharm. Pharm. Sci. 6 (2014) 20–23.
[17] M.I. Choudhary, M. Atif, S.A. Ali Shah, S. Sultan, S. Erum, S.N. Khan, Atta-Ur-Rahman, Biotransformation of Dehydroabietic acid with microbial cell cultures and α-Glucosidase inhibitory activity of resulting metabolites, Int. J. Pharm. Pharm. Sci. 6 (2014) 375–378.
[18] S.A.A. Shah, H.L. Tan, S. Sultan, M.A.B.M. Faridz, M.A.B.M. Shah, S. Nurfazilah, M. Hussain, Microbial-catalyzed biotransformation of multifunctional triterpenoids derived from phytonutrients, Int. J. Mol. Sci. 15 (2014) 12027–12060. doi:10.3390/ijms150712027.
[19] C. Djerassi, Chemical birth of the pill (2006) 290–298, https://doi.org/10.1016/j.ajog.2005.06.009.
[20] Toshiyuki Minami, Keiji Kosugi, Izumi Suganuma, Kaoruko Yamanaka, Izumi Kusuki, Tatsuya Oyama, Jo Kitawaki, Antiproliferative and apoptotic effects of norethisterone on endometriotic stromal cells in vitro, European Journal of Obstetrics & Gynecology and Reproductive Biology 166 (1) (2013) 76–80, https://doi.org/10.1016/j.ejogrb.2012.08.023.
[21] Salndave B. Skosana, John G. Woodland, Meghan Cartwright, Kim Enfield, Maleshigo Komane, Renate Louw-du Toit, Zephne van der Spuy, Chanel Avenant, Donita Africander, Karl-Heinz Storbeck, Janet P. Hapgood, Differential metabolism of clinically-relevant progestogens in cell lines and tissue: Implications for biological mechanisms, The Journal of Steroid Biochemistry and Molecular Biology 189 (2019) 145–153, https://doi.org/10.1016/j.jsbmb.2019.02.010.
[22] Takeshi Kaizuka, Hideaki Morishita, Yutaro Hama, Satoshi Tsukamoto, Takahide Matsui, Yuichiro Toyota, Akihiko Kodama, Tomoaki Ishihara, Tohru Mizushima, Noboru Mizushima, An Autophagic Flux Probe that Releases an Internal Control, Mol. Cell 64 (4) (2016) 835–849, https://doi.org/10.1016/j.molcel.2016.09.037.
[23] C. Su, N. Rybalchenko, D.A. Schreihofer, M. Singh, B. Abbassi, R.L. Cunningham, Cell Models for the Study of Sex Steroid Hormone Neurobiology, J Steroids Horm. Sci. 2 (2011), https://doi.org/10.4172/2157-7536.S2-003.
[24] J. Cummings, G. Lee, A. Ritter, K. Zhong, Alzheimer ' s disease drug development pipeline : 2018, Alzheimer's Dement. Transl. Res. Clin. Interv. 4 (2018) 195–214. doi:10.1016/j.trci.2018.03.009.
[25] Andrea Haake, Kevin Nguyen, Lauren Friedman, Binu Chakkamparambil, George T Grossberg, An update on the utility and safety of cholinesterase inhibitors for the treatment of Alzheimer's disease, Expert Opinion on Drug Safety 19 (2) (2020) 147–157, https://doi.org/10.1080/14740338.2020.1721456.
[26] G.L. Ellman, K.D. Courtney, V.J. Andres, R.M. Featherstone, A NEW AND RAPID COLORIMETRIC OF ACETYLCHOLINESTERASE DETERMINATION, Biochem. Pharmacol. 7 (1961) 88–95.
[27] Asokkumar Kuppusamy, Madeswaran Arumugam, Sonia George, Combining in silico and in vitro approaches to evaluate the acetylcholinesterase inhibitory profile of some commercially available flavonoids in the management of Alzheimer's disease, Int. J. Biol. Macromol. 95 (2017) 199–203, https://doi.org/10.1016/j.ijbiomac.2016.11.062.
[28] M.E. García, J.L. Borioni, V. Cavallaro, M. Puiatti, A.B. Pierini, A.P. Murray, A. B. Peñéñory, Solanocapsine derivatives as potential inhibitors of acetylcholinesterase : Synthesis, molecular docking and biological studies, Steroids 104 (2015) 95–110, https://doi.org/10.1016/j.steroids.2015.09.001.
[29] Lihu Zhang, Dongdong Li, Fuliang Cao, Wei Xiao, Linguo Zhao, Gang Ding, Zhen zhong Wang, Identification of Human Acetylcholinesterase Inhibitors from the Constituents of EGb761 by Modeling Docking and Molecular Dynamics Simulations, CCHTS 21 (1) (2018) 41–49, https://doi.org/10.2174/1386207320666171123201910.
[30] N.N.S. Silva, J.R.A. Silva, C.N. Alves, E.H.A. Andrade, J.K.R. da Silva, J.G.. Maia, Acetylcholinesterase Inhibitory Activity and Molecular Docking Study of 1-Acetylcholinesterase Inhibitory Activity and Molecular Docking Study of 1-Nitro-2-Phenylethane , the Main Constituent of Aniba canelilla Essential Oil, Chem Biol Drug Des. 84 (2014) 192–198. doi:10.1111/cbdd.12304.

[31] D.M. Quinn, Acetylcholinesterase: Enzyme Structure, Reaction Dynamics, and Virtual Transition States, (1987).
[32] Michal Harel, Daniel M. Quinn, Haridasan K. Nair, Israel Silman, Joel L. Sussman, The X-ray Structure of a Transition State Analog Complex Reveals the Molecular Origins of the Catalytic Power and Substrate Specificity of Acetylcholinesterase, J. Am. Chem. Soc. 118 (10) (1996) 2340–2346, https://doi.org/10.1021/ja952232h.
[33] S. Simeon, N. Anuwongcharoen, W. Shoombuatong, A.A. Malik, V. Prachayasittikul, J.E.S. Wikberg, C. Nantasenamat, Probing the origins of human acetylcholinesterase inhibition via QSAR modeling and molecular docking, PeerJ. 4 (2016) e2322. doi:10.7717/peerj.2322.